

# Vibration Mode Interaction in the Raman Spectra of Poly(1,6-bis[*N*-carbazolyl]-2,4-hexadiyne)

David Bloor\*

Department of Physics, University of Durham, South Road, Durham DH1 3LE, UK

Thomas Fehn†

Lehrstuhl für Experimentalphysik II, University of Bayreuth, D-95440 Bayreuth, Germany

Received February 23, 1999; Revised Manuscript Received August 24, 1999

**ABSTRACT:** The Raman spectrum of the polydiacetylene, poly(1,6-bis[*N*-carbazolyl]-2,4-hexadiyne), has been reexamined and analyzed in terms of the resonant interaction of backbone and side-group vibration modes. Fourier transform infrared Raman spectra have been recorded for partially and fully polymerized samples. These data complement earlier studies of the resonance-Raman spectra of partially polymerized crystals conducted at low temperatures. The multi-peaked spectrum, which is observed in the vicinity of the stretching vibration of the backbone carbon double bond, is analyzed utilizing these results. A model that incorporates the resonant interaction of the carbon double-bond mode with three vibrational modes of the carbazolyl side groups is shown to provide a good fit to the available experimental data.

## I. Introduction

The polydiacetylenes (PDAs) are a unique class of conjugated polymers that are obtained by the solid-state polymerization of substituted diacetylene monomers.<sup>1,2</sup> The lattice packing essential for solid-state polymerization to occur can be achieved for a variety of substituent groups.<sup>2</sup> Some examples of the chemical structures of the polymers obtained are shown in Figure 1. These polymers have morphologies that range from fully extended chains aligned in macroscopic single crystals to random chains in either solution or amorphous solids. They provide a model system for the study of the structure–property relationships of conjugated polymers. Raman spectroscopy has proved to be a particularly useful tool in the study of these and other conjugated polymers.<sup>3</sup> This is because the Raman spectra of conjugated polymers are dominated by the vibration modes of the conjugated backbone.<sup>3</sup> For visible excitation wavelengths this is due to a large resonant enhancement of the backbone modes. For infrared excitation the Raman scattering cross section is largest for terms involving the electron vibration coupling of the extended  $\pi$ -electron system.<sup>4</sup> Hence, at first sight the resonance Raman and FTIR spectra are very similar in appearance.<sup>5–8</sup> The latter, however, lack the overtone and combination vibration peaks that appear to very high frequency in resonance Raman spectra. They also exhibit numerous weaker features that are less obvious in the resonance Raman spectra.

For these reasons the typical Raman spectrum for a PDA has four intense lines, e.g., for PDA-pTS (see Figure 1) at ca. 950, 1200, 1480, and 2080  $\text{cm}^{-1}$ . These can be assigned on the basis of a simple force constant model<sup>9</sup> to motions involving principally bond bending about the triple bond (950  $\text{cm}^{-1}$ ) and the double bond (1200  $\text{cm}^{-1}$ ) and bond stretching of the double bond (1480  $\text{cm}^{-1}$ ) and the triple bond (2080  $\text{cm}^{-1}$ ). The frequencies of these lines are determined by the precise

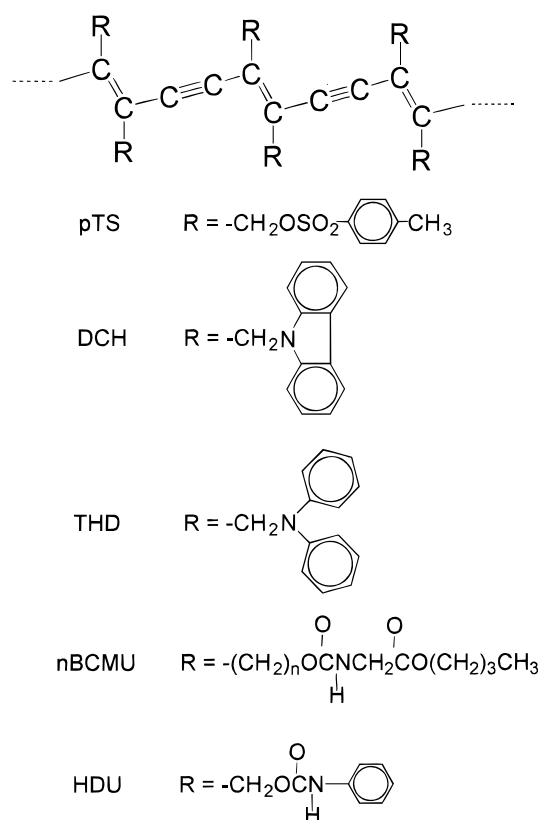


**Figure 1.** Chemical structures of polydiacetylenes prepared by solid-state polymerization and referred to in the text.

geometry of the polymer backbone and in consequence are affected by temperature, pressure, and tensile forces.<sup>3,10,11</sup> Raman spectroscopy has, therefore, provided a powerful tool for the study of polymer conformation and of the effects of external forces and environment on polymer structure. Recent examples of studies of PDAs include observation of the effects of high pressure on single crystals,<sup>12</sup> of disorder in solutions and solvent-cast films,<sup>13</sup> and of tensile forces on PDA chains in copolymers and blends.<sup>14,15</sup>

\* Corresponding author. E-mail david.bloor@durham.ac.uk.

† Permanent address: Gsänger Optoelektronik GmbH & Co. Kh, 82152 Planegg, Germany.

Although in general the side-group vibrations contribute only weak features to the Raman spectrum, there are two situations where side-group vibrational modes can produce strong spectral features. First, a resonant interaction between one of the strong backbone modes and a side-group mode, which is weakly active, will produce mixed modes, both of which have intense Raman activity. Whereas the side-group mode is an overtone or combination vibration, this is a classical Fermi resonance. Resonant interaction has been unambiguously observed for PDA-pTS, where a side-group  $\text{CH}_2$  mode couples with the double-bond stretching mode.<sup>16,17</sup> Second, even in the absence of a resonant interaction, a side-group mode may, through mechanical coupling to the backbone, produce sufficient amplitude of motion on the polymer backbone to give an observable Raman line.<sup>18</sup> This nonresonant coupling has been suggested as the origin of some medium-strength Raman lines, which occur when the side-group and backbone modes are not close in frequency, e.g., for the nBCMUs.<sup>7,8</sup>

The polymer obtained from 1,6-bis[*N*-carbazolyl]-2,4-hexadiyne (PDA-DCH) is unusual in having a Raman spectrum with three strong and one weak line in the region of the carbon double-bond stretching mode.<sup>3,7,19–21</sup> On the basis of a study of the low-temperature Raman spectra of partially polymerized crystals, these lines were attributed to a resonant interaction of the backbone mode with several side-group modes.<sup>22</sup> Subsequently, other groups reported little change in the appearance of the Raman spectrum of polymer crystals between 1400 and 1500  $\text{cm}^{-1}$  as a function of either tensile stress or temperature.<sup>7,21</sup> Furthermore, an analysis of the tensile stress data based on the resonant interaction of two modes gave only a modest fit.<sup>21</sup> Dyer et al.<sup>7</sup> therefore concluded, on the basis of this evidence and the negligible temperature dependence of the Raman spectrum, that the additional features in the Raman spectra of PDA-DCH were not due to a resonant interaction. However, neither stress nor changes in temperature produce as large a deformation of the polymer backbone as that imposed by the monomer matrix at low levels of conversion to polymer. In ideal cases the solid-state polymerization of PDAs proceeds via a single-phase solid solution of polymer in the monomer matrix.<sup>2</sup> This is the situation for DCH at low conversion when the polymer chains exist in a lattice with a repeat distance of 0.455 nm compared to an equilibrium repeat distance of 0.491 nm in the fully  $\gamma$ -ray polymerized material.<sup>23,24</sup> In addition, the cell dimension along the chain axis in the partially polymerized monomer is further reduced to 0.42 nm below a phase transition at 142 K.<sup>24,25</sup>

The study reported here was undertaken in order to resolve this controversy and establish the exact nature of the interaction of the side-group and polymer backbone vibration modes in PDA-DCH. This involved measurement of the FTIR–Raman spectra of partially polymerized monomer crystals, a reexamination of the low-temperature Raman data, and detailed modeling of the resonant interaction of the backbone vibration mode with three side-group vibration modes.

## II. Experimental Section

1,6-Bis[*N*-carbazolyl]-2,4-hexadiyne was prepared as described previously.<sup>25</sup> Monomer single crystals were grown from toluene solution. Rapid cooling yielded fine needlelike colorless crystals with dimensions of ca.  $0.2\text{--}0.3 \times 20\text{--}30$  mm. Slow

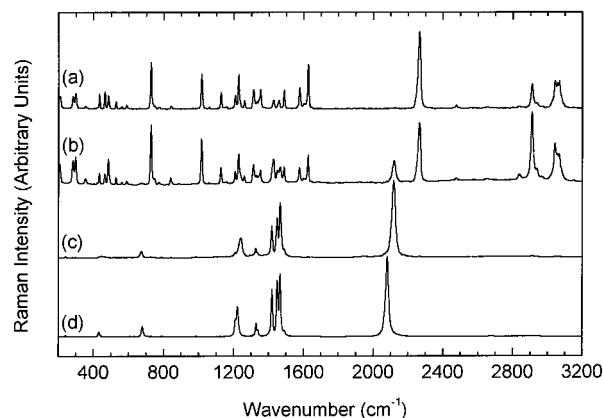


**Figure 2.** FTIR–Raman spectra of (a) randomly oriented monomer crystals, (b) a monomer crystal containing ca. 1% polymer, (c) a  $\gamma$ -ray-irradiated monomer crystal (dose 153.3 kGy), and (d) a polymer crystal obtained by  $\gamma$ -ray irradiation. The exciting radiation was polarized parallel to the polymer chain axis for (b), (c), and (d).

cooling provided crystals with cross sections up to 1–2 mm. Samples were polymerized by  $^{60}\text{Co}$   $\gamma$ -ray irradiation with doses of 54.8, 105.4, 150.1, and 153.3 kGy at Gammaster München Produktveredelungs GmbH. Using the data of ref 24, these doses correspond to conversion to polymer of ca. 0.5, 1.5, 10, and 15%, respectively. Samples were also available in which a low level of polymer had been produced during storage at room temperature for a period in excess of 10 years. The polymer content was estimated by comparing the color of these samples with that of the  $\gamma$ -ray-irradiated samples.

Raman spectra were recorded with a resolution of 4  $\text{cm}^{-1}$  on a Bruker IFS 55-FRA 106 FTIR–Raman spectrometer with an Adlas 300 Nd:YAG laser excitation source and Ge detector cooled with liquid nitrogen. A high signal-to-noise ratio was obtained by averaging between 20 and 200 interferometer scans depending on the strength of the Raman scattering. Resonance Raman spectra were recorded as described in the literature.<sup>17,22</sup>

Modeling was carried out with Mathsoft Inc., Mathcad Plus 6.0 computational software, which provides routines for the evaluation of eigenvalues and eigenvectors of matrices.

## III. Results and Discussion

FTIR–Raman spectra for four different samples of DCH are shown in Figure 2. The spectrum of a mat of freshly recrystallized monomer has a rich spectrum with a clear separation of high-frequency  $-\text{CH}$  stretching vibrations, a strong triple-bond stretching vibration at 2266  $\text{cm}^{-1}$ , and many lines below 1626  $\text{cm}^{-1}$  associated with the terminal groups (see Figure 2a). An old sample with a blue coloration (ca. 1% polymer) shows the monomer lines and in addition lines due to the polymer present in the monomer crystal. These occur at 2121  $\text{cm}^{-1}$  for the triple-bond stretching vibration and between 1400 and 1500  $\text{cm}^{-1}$  in the region of the double-bond stretching vibration. Other polymer lines are just discernible at lower frequencies but are obscured by the stronger monomer lines. This spectrum, Figure 2b, was recorded with the exciting radiation polarized parallel to the crystallographic *b*-axis,<sup>24</sup> i.e., parallel to the polymer chain axis. This accounts for the differences in relative amplitudes of the monomer lines in the spectra in Figure 2a,b. The polymer lines are absent from the spectrum of the old sample obtained with the exciting radiation polarized perpendicular to the polymer chain axis. Comparison of the spectra for the two polarizations allows approximate values for the frequency of some of the polymer lines to be deduced.

**Table 1. FTIR and Resonance Raman Line Frequencies for PDA-DCH Polymer in Partially and Fully Polymerized Crystals and for Polymer Extracted from Partially Polymerized Monomer (Unit  $\text{cm}^{-1}$ , Values  $\pm 2 \text{ cm}^{-1}$ )**

FTIR Raman						resonance Raman		
polymer			partially polymerized			polymer	partially polymerized	
ref 7	this work crystal	this work extracted	stored sample ca. 1% polymer <sup>a</sup>	stored sample ca. 10% polymer	$\gamma$ -irradiated 105.4 kGy	ref 19	at 150 K <sup>b</sup>	at 83 K <sup>b</sup>
2081	2081	2079	2121	2118	2118	2089	2126	2144
1492	1492	1492	1492	1492	1492		1492	1508
1466	1466	1468	1468	1468	1468	1472	1471	1493
1450	1450	1450	1450	1450	1450	1456	1453	1458
1420	1421	1421	~1420	1419	1419	1426	1422	1427
1340								
1329	1328	1329		1326	1327	1333		
1222	1222	1223		1236	1242	1226	1243	1248
1211						1217		
988	988	985			985			983
678	679	679		673	673	682	672	664
432	432	434		442		437		

<sup>a</sup> Values for carbon double-bond region estimated; see text. <sup>b</sup> Unpublished data, ref 22.

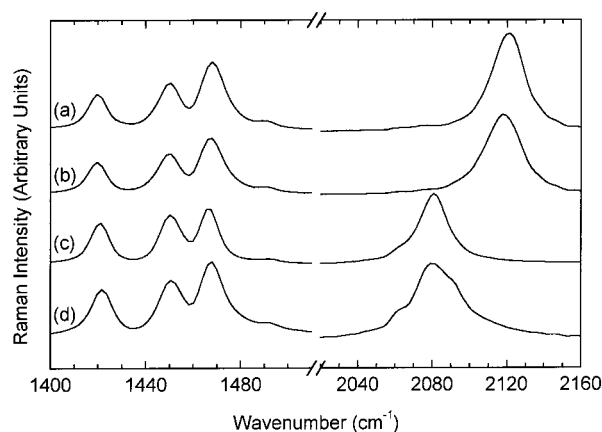


**Figure 3.** FTIR-Raman spectra in the region of the double- and triple-bond stretching vibrations for  $\gamma$ -ray-irradiated monomer crystals with doses of (a) 54.8 kGy and (b) 153.3 kGy, (c) a polymer crystal, and (d) polymer extracted from partially polymerized monomer. The exciting radiation was polarized parallel to the polymer chain for (a), (b), and (c).

For  $\gamma$ -ray-irradiated monomer at a dose of 153.3 KGy (ca. 15% polymer) the parallel polarized Raman spectrum is dominated by the polymer (see Figure 2c). The spectrum is very similar to that of a crystal fully polymerized by  $\gamma$ -ray irradiation (Figure 2d). The lines at ca. 2100 and 1220  $\text{cm}^{-1}$  become narrower and shift to lower frequency in the fully polymerized sample. However, the three strong lines between 1400 and 1500  $\text{cm}^{-1}$  are relatively unaffected by the change in polymer conformation during polymerization. This is shown in greater detail in Figure 3, where the ranges 1400–1500 and 2020–2160  $\text{cm}^{-1}$  are shown on an enlarged scale. The spectra shown in Figure 3 are for  $\gamma$ -irradiated monomer at doses of (a) 54.8 KGy (ca. 0.5% polymer) and (b) 153.3 KGy (ca. 15% polymer), (c) a fully polymerized crystal, and (d) polymer extracted from monomer crystals at ca. 5% polymer content. The carbon triple-bond stretching vibration shows a small shift in frequency between (a) and (b) and a large downshift for the polymer. The spectrum of Figure 3d shows that the polymer extracted from partially polymerized monomer relaxes to a structure close to that of the fully polymerized crystal. However, the complex line shape indicates that the polymer with different backbone structures is also produced during the process of extraction. Despite the large shift in the triple-bond stretching mode frequency during polymerization, the lines in the

**Table 2. Strain-Induced Shifts in the Vibration Frequencies for PDA-DCH and PDA-pTS (Unit  $\text{cm}^{-1}/\%$  Strain)**

vibration	PDA-DCH	PDA-pTS	
	tensile strain (ref 21)	tensile strain (ref 16)	thermal polym (ref 17)
triple-bond stretch	–17	–20.5	–23
double-bond stretch	–4 <sup>a</sup>	–8 <sup>a</sup>	–8 <sup>a</sup>
double-bond bend	–10	–10	
triple-bond bend		+0.5	

<sup>a</sup> Estimated after allowing for mode interaction.

vicinity of the carbon double-bond stretching vibration have only small frequency shifts and modest changes in relative intensity. The frequencies of the polymer Raman lines are collected in Table 1.

The frequency shifts in the polymer vibrations during polymerization can be compared with the shifts produced by tensile strain in PDA-DCH<sup>21</sup> and PDA-pTS<sup>16</sup> and during polymerization of PDA-pTS.<sup>17</sup> The data are collected in Table 2. Extension of the polymer chain results in a reduction of the frequencies of the double-bond stretching and bending modes and the triple-bond stretching mode. The triple-bond bending mode is only weakly affected. The variation of triple- and double-bond frequencies as a function of temperature is similar for HDU<sup>26</sup> and for PDA-pTS.<sup>10</sup> The ratio of the shifts for the triple- and double-bond vibrations is ca. 1:0.3.<sup>13</sup> A larger ratio has been reported for PDA-DCH, but the value used for the shift in the double-bond stretching mode is an estimate deduced from fitting the experimental data with an interaction between the backbone mode and a single side-group mode.<sup>21</sup> The inadequacy of this analysis was noted by Wu et al., and this accounts for the discrepancy between the data for PDA-pTS and PDA-DCH listed in Table 2. At low levels of conversion to polymer the PDA-DCH chains in the monomer lattice are confined to a unit cell of size 0.455 nm compared to an equilibrium backbone repeat distance of 0.491 nm, i.e., are compressed by ca. 8%.<sup>23,24</sup> The triple-bond mode is shifted up in frequency by 40  $\text{cm}^{-1}$  relative to fully converted polymer (cf. Table 1). The shift is in the correct direction but is smaller than expected from the tensile strain data. However, the effective strain is outside the range where the response to strain is linear.<sup>16</sup> Furthermore, the strain is not uniaxial in this case, and there will certainly be dimensional changes perpendicular to the chain axis. The effect of lateral deformation has been observed



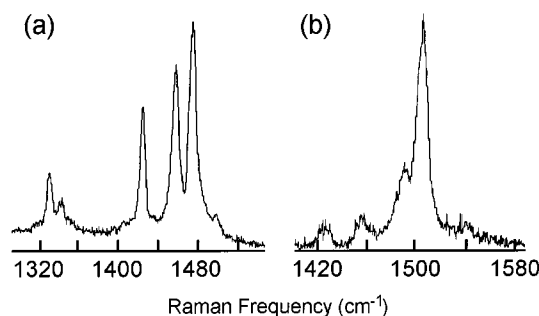


**Figure 4.** Resonance Raman spectra of a partially polymerized crystal of DCH monomer, containing less than 5% polymer, recorded above and below the solid-state phase transition of the monomer at (a) 150 and (b) 83 K, respectively.

during the polymerization of PDA-pTS.<sup>17</sup> A shift of ca.  $20\text{ cm}^{-1}$  is observed for the double-bond bending mode, which is also smaller than predicted for uniaxial compression. However, no comparable shifts are apparent in the region of the double-bond stretching mode between  $1400$  and  $1500\text{ cm}^{-1}$ .

That the double-bond stretching vibration interacts with more than one side-group mode is shown conclusively by the Raman spectra of partially polymerized crystals recorded below the  $142\text{ K}$  phase transition.<sup>22</sup> Resonance Raman spectra in the double-bond stretching mode region recorded at  $150$  and  $83\text{ K}$  are shown in Figure 4. The former is very similar to that of the partially polymerized crystals at room temperature (see Figure 3 and Table 1). However, below the phase transition the double-bond vibration appears as a single line at  $1508\text{ cm}^{-1}$ . The previously intense lines below  $1500\text{ cm}^{-1}$  now appear as weak features. Since the phase transition produces large changes in the unit cell dimensions and angles, the observed shifts cannot be compared with the results obtained under tensile strain. The triple-bond frequency increases by ca.  $25\text{ cm}^{-1}$  from its value at room temperature while it is obvious that there is a larger shift for the double-bond vibration. At room temperature it must be in the vicinity of the lines at  $1450$  and  $1468\text{ cm}^{-1}$ , implying an upward shift of over  $40\text{ cm}^{-1}$  for the polymer in the monomer below  $142\text{ K}$ . This shift is approximately twice that of the triple bond and is indicative of the complex nature of the deformation that occurs at the phase transition.

The spectra shown in Figure 4 suggest that there is an interaction between the carbon double-bond stretching vibration and at least two side-group vibration modes. The  $83\text{ K}$  spectrum, Figure 4b, indicates that the unperturbed side-group vibration frequencies are at ca.  $1430$  and  $1460\text{ cm}^{-1}$ , i.e., slightly higher than the observed frequencies of the weak lines at  $1427$  and  $1458\text{ cm}^{-1}$ . There is a third vibration at ca.  $1492\text{ cm}^{-1}$  that appears in all the Raman spectra. The low intensity of this line indicates that the interaction with the backbone mode is weak. A number of features have been observed in the monomer Raman spectrum and the infrared spectrum of carbazole with similar frequencies. Bree and Zwarich<sup>27,28</sup> reported  $B_2$  modes for carbazole at  $1490$ ,  $1452$ , and  $1422\text{ cm}^{-1}$ . Lines appear at these frequencies in the FTIR–Raman spectrum of the PDA-DCH monomer, the latter two lines as shoulders on more intense peaks at  $1460$  and  $1430\text{ cm}^{-1}$ . The close coincidence of the monomer Raman lines at  $1490$ ,  $1460$ , and  $1430\text{ cm}^{-1}$  with the estimated frequencies of the interacting modes is suggestive that they are due to the

same side-group vibrations. There are also numerous low-frequency features in the monomer Raman spectrum and the carbazole infrared spectrum that could produce harmonics and combinations of the right frequency to interact with the backbone double-bond vibration. It can be seen from Figure 1 that the only features retained in the polymer spectrum with any resemblance to the monomer spectrum are those between  $1400$  and  $1500\text{ cm}^{-1}$ . Thus, Raman activity is transferred from the backbone double-bond vibration to the side-group modes. Although precise identification of the side-group modes involved is not possible, comparison with the Raman spectrum of PDA-THD (see Figure 1), which has a single carbon double-bond stretching line,<sup>29</sup> shows that they must originate from the carbazole group. It is, however, clear that the interactions are resonant.

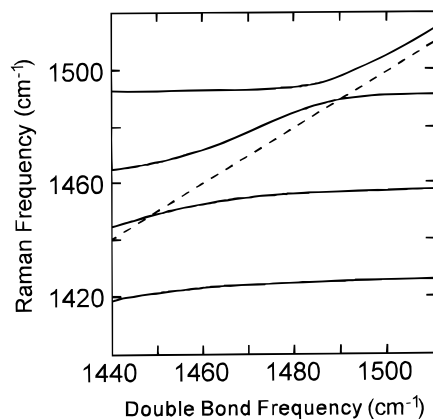
Modeling the mode interaction is not as straightforward as for PDA-pTS, where a single side-group mode is involved. The problem is compounded by the extreme conditions that the polymer chain is subject to in the partially polymerized crystals, particularly at low temperatures. This can be seen in Figures 3 and 4. The line width of the carbon triple-bond line in the polymer is  $16\text{ cm}^{-1}$  full width at half-maximum height, in agreement with Dyer et al.<sup>7</sup> In the  $\gamma$ -ray polymerized monomer containing ca.  $15\%$  polymer, the line width is  $25\text{ cm}^{-1}$ . The additional width can be attributed to inhomogeneous broadening due to a distribution of local strain in the partially polymerized crystal. Such line broadening has been observed in PDA-pTS where the dimensional change on polymerization is less than that for PDA-DCH.<sup>17</sup> At  $150\text{ K}$  the line width of the lines between  $1400$  and  $1500\text{ cm}^{-1}$  falls to about half the room-temperature value, cf. ca.  $5\text{ cm}^{-1}$  from ca.  $10\text{ cm}^{-1}$ . However, the double-bond line at  $83\text{ K}$  has a line width of ca.  $10\text{ cm}^{-1}$ , double that at  $150\text{ K}$ . Thus, the distribution of local strain has been increased by the large dimensional changes that occur at the phase transition.<sup>24,25</sup> For PDA-pTS the dimensional changes during polymerization caused a detectable change in the coupling constant between the backbone and side-group vibration modes of ca.  $20\%$ .<sup>17</sup> The much larger dimensional changes in PDA-DCH are likely to produce somewhat larger changes in the mode coupling constants.

In view of the very different crystal environments, a simple model with fixed coupling constants cannot be expected to give a perfect fit to the data for partially polymerized crystals reported here and the temperature and strain dependence reported previously.<sup>7,21</sup> However, in the absence of any means of estimating the changes in mode coupling constants, it is the best model available. Comparison of this simple model and the experimental data can, however, help demonstrate that a complex resonant interaction occurs in PDA-DCH.

The interaction matrix for a double-bond vibration of continuously variable frequency with fixed modes at  $1492$ ,  $1459$ , and  $1429\text{ cm}^{-1}$  was solved using the eigenvalue and eigenvector routines provided in the Mathcad Plus 6 software package. The off-diagonal coupling constants that gave a reasonable approximation to the experimental data were  $4$ ,  $8$ , and  $15\text{ cm}^{-1}$  for the double-bond with the three fixed modes at  $1492$ ,  $1459$ , and  $1429$ , respectively, and  $4.5\text{ cm}^{-1}$  between the modes at  $1459$  and  $1429\text{ cm}^{-1}$ . These values of the coupling constants are comparable with the value of  $7\text{ cm}^{-1}$

**Table 3. Comparison of the Observed and Calculated Raman Frequencies ( $\text{cm}^{-1}$ ) for PDA-DCH in the Double-Bond Stretching Vibration Region (1400–1500  $\text{cm}^{-1}$ )**

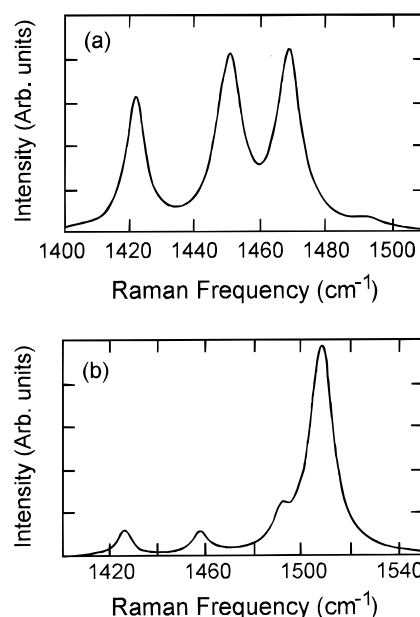
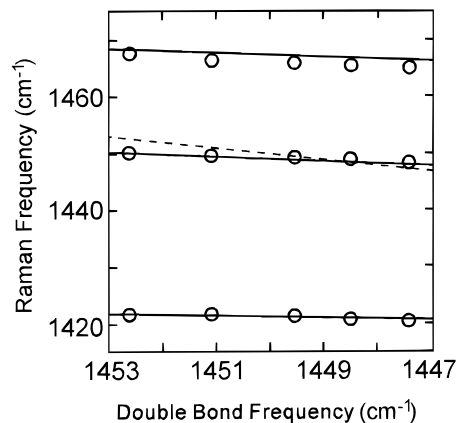
polymer		$\gamma$ -irradiated ca. 1.5% polymer		partially polymerized 150 K		partially polymerized 83 K	
Raman data <sup>a</sup>	model	Raman data <sup>a</sup>	model	Raman data <sup>b</sup>	model	Raman data <sup>b</sup>	model
1492	1492	1492	1492	1492	1493	1508	1508
1466	1466	1468	1468	1471	1471	1493	1491
1450	1448	1450	1450	1453	1452	1458	1458
1421	1420	1419	1422	1422	1423	1427	1426

<sup>a</sup> FTIR Raman. <sup>b</sup> Resonance Raman.**Figure 5.** Raman line frequencies in the range 1400–1520  $\text{cm}^{-1}$  as a function of a variable carbon double-bond stretching vibration frequency calculated as described in the text. The dash line shows the position of the unperturbed double-bond vibration.

observed for PDA-pTS.<sup>16</sup> The calculated variation of the Raman line frequencies is shown as a function of the unperturbed, continuously variable double-bond mode frequency in Figure 5. The dash line shows the position of the latter. Values obtained with this calculation are compared with the experimental data in Table 3. Relative intensities were calculated from the fractional double-bond mode character for each eigenvalue. The spectral profile was calculated as a sum of Lorentzian lines. For lines of equal width the fit to the observed spectra was reasonable but was improved by using slightly different line-width parameters. Those used to calculate the spectral profiles shown in Figure 6 were 9, 8, 9, and 7  $\text{cm}^{-1}$  for the double-bond, 1492, 1459, and 1429  $\text{cm}^{-1}$  modes, respectively. The width of the double bond was increased to 12  $\text{cm}^{-1}$  for Figure 6b to allow for the strain broadening observed at 83 K. The representation of the spectra of Figures 3 and 4 with this set of parameters is good.

This model explains the small changes observed in the 1400–1500  $\text{cm}^{-1}$  spectral region as a function of strain and temperature. Figure 7 compares the experimental data of Wu et al.<sup>21</sup> with the Raman frequencies calculated for an appropriate change in the backbone double-bond mode frequency. This was estimated from the experimentally observed change in frequency of the triple-bond stretching vibration of 16  $\text{cm}^{-1}$  for a stress of 0.4 GPa.<sup>21</sup> Comparison with PDA-pTS indicates that the unperturbed double bond will shift by a maximum of 6  $\text{cm}^{-1}$  (cf. Table 2).<sup>13</sup> Over this range the calculated line frequencies are close to those reported by Wu et al. The calculated change in relative integrated intensity of the two lowest frequency lines, ca. 35%, is also close to the experimental value.

Dyer et al.<sup>7</sup> ruled out resonant interaction, including Fermi resonance, involving the double-bond stretching mode because of the absence of significant changes in

**Figure 6.** Calculated Raman spectral profiles in the range 1400–1550  $\text{cm}^{-1}$  for carbon double-bond stretching vibration frequencies of (a) 1453 and (b) 1502  $\text{cm}^{-1}$ . Parameters used in the calculation are given in the text.**Figure 7.** Calculated Raman line frequencies as a function of a variable double-bond stretching vibration frequency over a range commensurate with that produced by tensile stress. Experimental data from Wu et al.<sup>21</sup> are plotted as open circles. The dash line shows the position of the unperturbed double-bond vibration.

the polymer Raman spectrum between 1400 and 1500  $\text{cm}^{-1}$  at room temperature and 150 K. However, examination of their data reveals that the spectral profiles are not identical. Unfortunately, the data presented in ref 7 are insufficient to enable a precise comparison to be made with the model calculation. Dyer et al. do not list the line frequencies observed at 150 K so that the shift in the triple-bond frequency is not available. However, for PDA-pTS between 300 and 150 K the

triple- and double-bond frequencies increased by 5 and  $1.5\text{ cm}^{-1}$ , respectively.<sup>10</sup> The triple-bond vibrational frequency is less sensitive to strain in PDA-DCH than PDA-pTS. Hence, the double-bond frequency is unlikely to shift by more than  $1\text{ cm}^{-1}$  between 300 and 150 K in PDA-DCH. Such a change produces a negligible shift in line frequencies (cf. Figure 7) and changes in relative line strength of at most 5%. The absence of striking changes in the polymer Raman spectrum at 150 K is, therefore, not at odds with the occurrence of resonant interaction between the carbon double-bond stretching mode and several side-group vibrational modes.

#### IV. Conclusions

The multicomponent Raman spectrum in the region of the backbone carbon double-bond stretching vibration of PDA-DCH has been attributed to either resonant interaction between this mode and side-group vibration modes<sup>22</sup> or side-group modes with a naturally large, nonresonant amplitude on the polymer backbone.<sup>7</sup> The former model is favored by the observation of a single strong Raman line in the spectrum of partially polymerized monomer below the 142 K crystallographic phase transition of the monomer. The spectrum observed in partially polymerized monomer and polymer crystals can be modeled by considering the resonant interaction of the backbone vibration with three side-group vibrations. Such a model was suggested by Wu et al.<sup>21</sup> but not implemented by them. Given the large changes in crystal structure between the monomer and polymer at room temperature and the monomer below 142 K, the mode interaction parameters in each of these situations will be different. However, a model using a single set of parameters gives a reasonable approximation to the observed line frequencies and spectral profiles. It also provides a reasonable fit to the spectra recorded under tensile stress reported by Wu et al.<sup>21</sup> This model also predicts the negligible temperature dependence of the polymer spectra observed by Dyer et al.<sup>7</sup> Thus, we conclude that the unusual, possibly unique, structure observed in the Raman spectrum of PDA-DCH is a consequence of the occurrence of simultaneous resonant interactions between several vibration modes.

**Acknowledgment.** D.B. thanks the Alexander von Humboldt Stiftung for the award of a Fellowship. The FTIR–Raman spectroscopy was performed during the tenure of this Fellowship at the University of Bayreuth. Professor M. Schwoerer is thanked for providing laboratory facilities and D. J. Ando and I. F. Chalmers are thanked for providing the PDA-DCH monomer and polymer.

#### References and Notes

- (1) Wegner, G. Z. *Naturforsch.* **1969**, *245*, 824–832.
- (2) Bloor, D. In *Developments in Crystalline Polymers II*; Bassett, D. C., Ed.; Applied Science Publishers: London, 1982; pp 151–193.
- (3) Batchelder, D. N.; Bloor, D. In *Advances in Infrared and Raman Spectroscopy*; Clark, R. J. H., Hester, R. E., Eds.; Wiley Heyden: Chichester, 1984; Vol. 2, pp 133–209.
- (4) Castiglioni, C.; Del Zoppo, M.; Zerbi, G. *J. Raman Spectrosc.* **1993**, *24*, 485–494.
- (5) Engert, C.; Materny, A.; Kiefer, W. *Chem. Phys. Lett.* **1992**, *198*, 395–399.
- (6) Shchegolikhin, A. N.; Lazareva, O. L. *Spectrochim. Acta A* **1997**, *53*, 67–79.
- (7) Dyer, C. D.; Hendra, P. J.; Maddams, W. F. *Spectrochim. Acta A* **1997**, *53*, 2323–2332.
- (8) Bloor, D. *Polymer* **1999**, *40*, 3901–3908.
- (9) Lewis, W. F.; Batchelder, D. N. *Chem. Phys. Lett.* **1978**, *60*, 232–237.
- (10) Cottle, A. C.; Lewis, W. F.; Batchelder, D. N. *J. Phys. C: Solid State Phys.* **1978**, *11*, 605–616.
- (11) Batchelder, D. N.; Kennedy, R. J.; Bloor, D.; Young, R. J. *J. Polym. Sci., Polym. Phys. Ed.* **1981**, *19*, 677–688.
- (12) Webster, S.; Batchelder, D. N. *Macromol. Symp.* **1994**, *87*, 177–185.
- (13) Campbell, A. J.; Davies, C. K. L.; Batchelder, D. N. *Macromol. Chem. Phys.* **1998**, *199*, 109–112.
- (14) Hu, X.; Stanford, J. L.; Young, R. J. *Polymer* **1994**, *35*, 80–85.
- (15) Lovell, P. A.; Stanford, J. L.; Wang, Y. F.; Young, R. J. *Macromolecules* **1998**, *31*, 842–849.
- (16) Batchelder, D. N.; Bloor, D. *J. Polym. Sci., Polym. Phys. Ed.* **1979**, *17*, 569–581.
- (17) Bloor, D.; Kennedy, R. J.; Batchelder, D. N. *J. Polym. Sci., Polym. Phys. Ed.* **1979**, *17*, 1355–1366.
- (18) Bloor, D.; Hersel, W.; Batchelder, D. N. *Chem. Phys. Lett.* **1977**, *45*, 411–414.
- (19) Elman, B. S.; Thakur, M. K.; Sandman, D. J.; Newkirk, M. A.; Kennedy, E. F. *J. Appl. Phys.* **1985**, *57*, 4996–5005.
- (20) Sandman, D. J.; Chan, Y. J.; Elman, B. S.; Velazquez, C. S. *Macromolecules* **1988**, *21*, 3112–3113.
- (21) Wu, G.; Tashiro, K.; Kobayashi, M. *Macromolecules* **1989**, *22*, 188–196.
- (22) Kennedy, R. J.; Chalmers, I. F.; Bloor, D. *Macromol. Chem. Rapid Commun.* **1980**, *1*, 357–361.
- (23) Apgar, P. A.; Yee, K. G. *Acta Crystallogr. B* **1978**, *34*, 957–959.
- (24) Enkelmann, V.; Leyrer, R. J.; Schleier, G.; Wegner, G. *J. Mater. Sci.* **1980**, *15*, 168–176.
- (25) Bloor, D.; Chalmers, I. F.; Kennedy, R. J.; Motevalli, M. *J. Mater. Sci.* **1985**, *20*, 674–681.
- (26) Mitra, V. K.; Risen, W. M., Jr.; Baughman, R. H. *J. Chem. Phys.* **1977**, *66*, 2731–2736.
- (27) Bree, A.; Zwarich, R. *J. Chem. Phys.* **1968**, *49*, 3344–3355.
- (28) Bree, A.; Zwarich, R. *Spectrochim. Acta A* **1971**, *27A*, 599–620.
- (29) Morrow, M. E.; White, K. M.; Eckhardt, C. J.; Sandman, D. *J. Chem. Phys. Lett.* **1987**, *140*, 263–269.

MA9902652